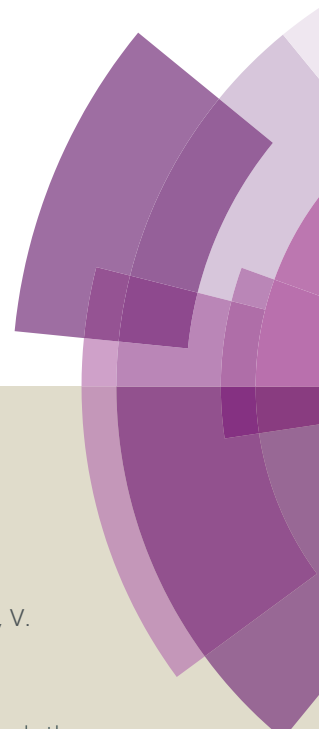
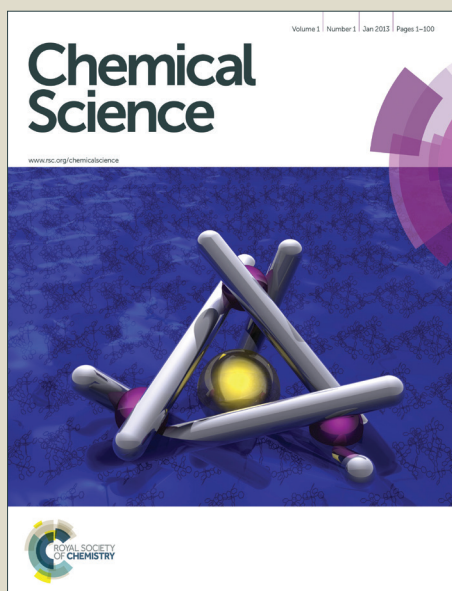


# Chemical Science

Accepted Manuscript



This article can be cited before page numbers have been issued, to do this please use: S. Wesselbaum, V. Moha, M. Meuresch, S. Brosinski, K. M. Thenert, J. Kothe, T. vom Stein, U. Englert, M. Hoelscher, J. Klankermayer and W. Leitner, *Chem. Sci.*, 2014, DOI: 10.1039/C4SC02087A.



This is an *Accepted Manuscript*, which has been through the Royal Society of Chemistry peer review process and has been accepted for publication.

*Accepted Manuscripts* are published online shortly after acceptance, before technical editing, formatting and proof reading. Using this free service, authors can make their results available to the community, in citable form, before we publish the edited article. We will replace this *Accepted Manuscript* with the edited and formatted *Advance Article* as soon as it is available.

You can find more information about *Accepted Manuscripts* in the [Information for Authors](#).

Please note that technical editing may introduce minor changes to the text and/or graphics, which may alter content. The journal's standard [Terms & Conditions](#) and the [Ethical guidelines](#) still apply. In no event shall the Royal Society of Chemistry be held responsible for any errors or omissions in this *Accepted Manuscript* or any consequences arising from the use of any information it contains.

Cite this: DOI: 10.1039/c0xx00000x

www.rsc.org/xxxxxx

## ARTICLE TYPE

Hydrogenation of Carbon Dioxide to Methanol using a Homogeneous Ruthenium-Triphos Catalyst: From Mechanistic Investigations to Multiphase Catalysis<sup>†</sup>Sebastian Wesselbaum,<sup>a</sup> Verena Moha,<sup>a</sup> Markus Meuresch,<sup>a</sup> Sandra Brosinski,<sup>a</sup> Katharina M. Thenert,<sup>a</sup> Jens Kothe,<sup>a</sup> Thorsten vom Stein,<sup>a</sup> Ulli Englert,<sup>b</sup> Markus Hölscher,<sup>a</sup> Jürgen Klankermayer,<sup>a\*</sup> and Walter Leitner<sup>a\*</sup>

Received (in XXX, XXX) Xth XXXXXXXXX 20XX, Accepted Xth XXXXXXXXX 20XX

DOI: 10.1039/b000000x

The hydrogenation of CO<sub>2</sub> to methanol can be achieved by a single molecular organometallic catalyst.

Whereas homogeneous catalysts were previously believed to allow the hydrogenation only *via* formate esters as stable intermediates, the present mechanistic study demonstrates that the multistep transformation can occur directly on the Ru-Triphos (Triphos = 1,1,1-tris(diphenylphosphinomethyl)ethane) centre. The cationic formate complex [(Triphos)Ru(η<sup>2</sup>-O<sub>2</sub>CH)(S)]<sup>+</sup> (S = solvent) was identified as key intermediate, leading to the synthesis of the analogous acetate complex as robust and stable precursor for the catalytic transformation. A detailed mechanistic study using DFT calculation shows that a sequential series of hydride transfer and protonolysis steps can account for the transformation of CO<sub>2</sub> *via* formate/formic acid to hydroxymethanolate/formaldehyde and finally methanolate/methanol within the coordination sphere of a single Ru-Triphos-fragment. All experimental results of systematic parameter optimisation are fully consistent with this mechanistic picture. Based on these findings, a biphasic system consisting of H<sub>2</sub>O und 2-MTHF was developed, where the active cationic Ru-complex resides in the organic phase for recycling and methanol is extracted with the aqueous phase.

## Introduction

The depletion of fossil carbon sources together with the increasing global energy consumption demand alternative ways for the sustainable production of fuels and chemicals. In this context, the usage of carbon dioxide (CO<sub>2</sub>) as alternative carbon source has seen renewed and increasing interest at the interface of the chemical and energy sector, as it is a readily available, non-toxic by-product of various large scale industries.<sup>1–11</sup> Particularly the effective hydrogenation of carbon dioxide to methanol could play an important role in supply chains with reduced carbon footprint economy, as methanol can serve as energy carrier and versatile basic chemical.<sup>12–15</sup> Today methanol is produced on megaton scale from fossil feedstock-based syngas (CO/H<sub>2</sub>).<sup>15, 16</sup> These processes utilise heterogeneous catalysts at elevated temperatures (200–300 °C) and pressures (50–100 bar).

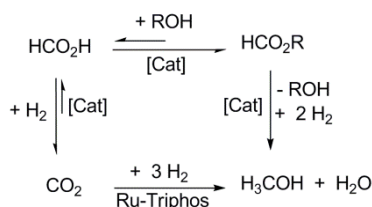
A certain percentage of CO<sub>2</sub> is added to the feedstock stream to balance the C/H ratio. The heterogeneously catalysed hydrogenation of pure CO<sub>2</sub> to methanol has been implemented capitalising on the specific regional energy and feedstock basis in Iceland, for example.<sup>17</sup> A detailed picture of the elementary steps and the role of the multi-component catalyst material have been elucidated for the classical Cu/ZnO/Al<sub>2</sub>O<sub>3</sub> systems, mapping out the complex series of bond cleavage and bond forming processes on the catalyst surface that enable the seemingly simple overall transformation of CO or CO<sub>2</sub> and hydrogen to methanol.<sup>18</sup>

In sharp contrast, the hydrogenation of CO<sub>2</sub> to methanol using a molecularly defined, single-site catalyst has remained elusive up to now. Tominaga *et al.* reported the formation of methanol besides methane and CO from CO<sub>2</sub> hydrogenation using Ru<sub>3</sub>(CO)<sub>12</sub> in the presence of alkaline iodides under harsh reaction conditions (240 °C, 80 bar). Under these conditions, CO<sub>2</sub> was reduced to CO followed by the hydrogenation of the CO to methanol and methane.<sup>19</sup> Later, the catalytic formation of methanol from CO<sub>2</sub> was reported with organometallic complexes using high energy reduction reagents such as boranes.<sup>20</sup> With hydrogen, indirect routes *via* conversion of CO<sub>2</sub>-derived intermediates like organic carbonates, carbamates, formate esters and ureas were proposed (see Scheme 1, upper pathway, for formate esters). The viability of this concept was first

<sup>a</sup> Institut für Technische und Makromolekulare Chemie, RWTH Aachen University, Worringerweg 1, 52074 Aachen, Germany. E-mail: jklankermayer@itmc.rwth-aachen.de; leitner@itmc.rwth-aachen.de

<sup>b</sup> Institut für Anorganische Chemie, RWTH Aachen University, Landoltweg 1, 52074 Aachen, Germany.

<sup>†</sup> Electronic Supplementary Information (ESI) available: [Experimental procedures, analytical data]. See DOI: 10.1039/b000000x/

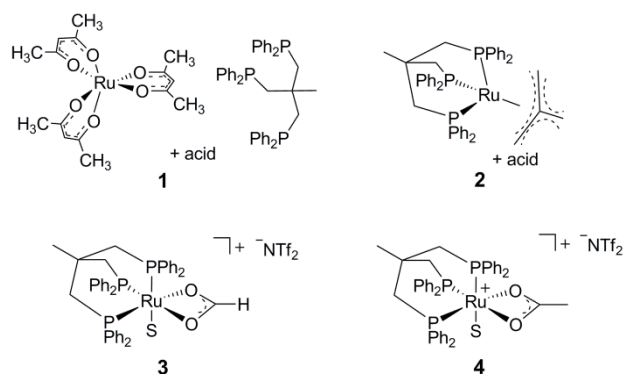


**Scheme 1** Hydrogenation of CO<sub>2</sub> to methanol via formate esters as proposed by Milstein *et al.*<sup>21</sup> and previously shown by Sanford/Huff<sup>23</sup> and Klankermayer/Leitner<sup>24</sup> (upper pathway), and hydrogenation of CO<sub>2</sub> to methanol without the need for an alcohol additive as shown in the present report (lower pathway).

demonstrated in the seminal work by Milstein *et al.*, who developed highly efficient Ruthenium(II) pincer complexes for the hydrogenation of these challenging substrates.<sup>21, 22</sup> Huff and Sanford reported a three step, one pot hydrogenation of CO<sub>2</sub> to methanol *via* methyl formate as intermediate using a combination of the Milstein catalyst with two other catalysts.<sup>23</sup>

Most recently, we were able to show that the sequential reduction *via* formate ester for the homogeneous hydrogenation of CO<sub>2</sub> to methanol could be achieved in a fully integrated reaction with a single molecular catalyst based on Ruthenium as central metal and the tridentate ligand Triphos (Triphos = 1,1,1-tris(diphenylphosphinomethyl)ethane).<sup>24</sup> The catalyst could be formed *in situ* from Ru(acac)<sub>3</sub> and Triphos **1** or using the readily accessible ruthenium(II)-complex [(Triphos)Ru(TMM)] **2** (TMM = trimethylenemethane) as precursor, both in the presence of an acid co-catalyst (Scheme 2).<sup>25–29</sup>

In the present report we disclose for the first time the hydrogenation of CO<sub>2</sub> to methanol using a single molecularly-defined homogeneous catalyst without the need for an alcohol additive (Scheme 1, lower pathway). This fundamental step forward was derived from comprehensive mechanistic investigations concerning the catalyst system **2** which led to the identification of the cationic formate complex [(Triphos)Ru(η<sup>2</sup>-O<sub>2</sub>CH)(S)]<sup>+</sup> (S = solvent) **3** as catalytically active intermediate in solution (Scheme 2). Based thereon, the analogous cationic acetate complex **4** was developed as pre-catalyst (Scheme 2). These molecular catalysts allow the homogeneously catalysed formation of methanol using CO<sub>2</sub> and H<sub>2</sub> as the sole feedstock with turnover frequencies in the same range as reported for the active sites of the heterogeneous systems. We also demonstrate



**Scheme 2** Catalyst precursors **1**, **2** and **4** (S = free coordination site or solvent) for the CO<sub>2</sub> hydrogenation to methanol and structure of the catalytically active intermediate **3** (S = solvent).

the possibility to separate and recycle these catalysts from the MeOH/water product mixture in a biphasic aqueous system using 2-methyl tetrahydrofuran (2-MTHF) as catalyst phase.

## Results and Discussion

### Basic reactivity and identification of the active species

Attempting to identify intermediates of the previously reported catalytic reaction sequence with catalyst **2**,<sup>24, 30</sup> multinuclear NMR experiments were carried out to monitor the formation of organometallic species upon stepwise addition of the required components. Thus, a solution of the precursor [(Triphos)Ru(TMM)] (**2**) and HNTf<sub>2</sub> (1 eq.) in *d*<sub>8</sub>-THF was pressurised with CO<sub>2</sub> (20 bar at r.t.) and H<sub>2</sub> (60 bar at r.t.), stirred for 1 h at 140 °C, and then transferred to a NMR tube for analysis. Unexpectedly, a sharp signal at 3.27 ppm in the <sup>1</sup>H-NMR spectrum indicated the catalytic formation of MeOH already in the absence of any alcohol additive with a TON of 35. Thus, one of the species formed under these conditions must be able to serve as catalyst for the hydrogenation of CO<sub>2</sub> to methanol. The <sup>31</sup>P{<sup>1</sup>H}-NMR spectrum of the clear, yellow solution obtained under these conditions is depicted in Figure 1, the corresponding <sup>1</sup>H, <sup>13</sup>C and 2D-correlation spectra are shown in the supporting information.

Formation of the cationic carbonyl complex [(Triphos)RuH(CO)<sub>2</sub>]<sup>+</sup> (**5**) was inferred from the characteristic set of a doublet (18.6 ppm, *J* = 28.7 Hz) and triplet (6.3 ppm, *J* = 28.7 Hz) in the <sup>31</sup>P{<sup>1</sup>H}-NMR.<sup>31</sup> Correlation with the hydride signal at δ = −6.7 ppm in the [<sup>1</sup>H, <sup>31</sup>P]-HMBC-NMR spectrum and ESI-MS analysis further confirmed this assignment. The content in solution was about 4 % according to the integral ratios in the <sup>31</sup>P{<sup>1</sup>H}-NMR spectrum. The formation of complex **5** corroborates the assumption of cationic complexes as catalytically active species. The carbonyl ligands are most likely formed by decarbonylation of intermediates on the pathway to methanol.<sup>28,32,33</sup> Supporting this hypothesis, **5** could be synthesised in pure form by stirring complex **2** together with 1 equivalent of HNTf<sub>2</sub> in ethyl formate and 60 bar H<sub>2</sub> in the absence of CO<sub>2</sub> for 24 hours at 140 °C. Testing the isolated

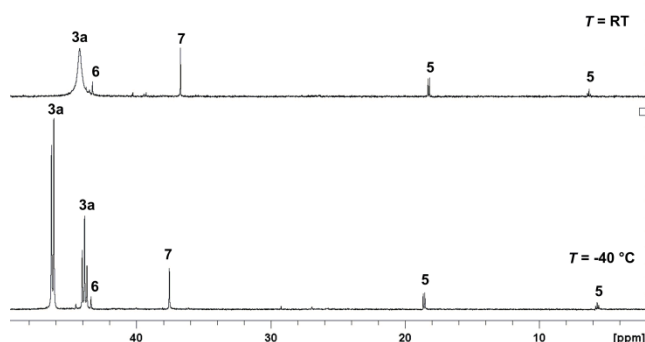


**Fig. 1** <sup>31</sup>P{<sup>1</sup>H}-NMR spectra (top: at r.t., bottom: at −40 °C) of the reaction solution after CO<sub>2</sub> hydrogenation to methanol (20 bar CO<sub>2</sub> + 60 bar H<sub>2</sub>, 140 °C, 1 h) with catalyst **2** (50 μmol) and HNTf<sub>2</sub> (1 eq.) in *d*<sub>8</sub>-THF (2 mL). **5** = [(Triphos)RuH(CO)<sub>2</sub>]<sup>+</sup>, **6** = [Ru<sub>2</sub>(μ-H)<sub>2</sub>(Triphos)<sub>2</sub>]<sup>+</sup>, **7** = [Ru<sub>2</sub>(Cl)<sub>3</sub>(Triphos)<sub>2</sub>]<sup>+</sup>, **3a** = [(Triphos)Ru(η<sup>2</sup>-O<sub>2</sub>CH)(THF)]<sup>+</sup>.

complex **5** for its catalytic activity in CO<sub>2</sub> hydrogenation in the absence of alcohol (standard conditions:  $V(\text{THF}) = 2.08 \text{ mL}$ ,  $c(\text{Ru}) = 12 \text{ mmol/L}$ , 1 eq. of  $\text{HNTf}_2$ ,  $p(\text{CO}_2) = 20 \text{ bar}$  at r.t.,  $p(\text{H}_2) = 60 \text{ bar}$  at r.t.,  $T = 140^\circ\text{C}$ ,  $t = 24 \text{ h}$ ) gave only a TON of 4, identifying the formation of **5** as a possible deactivation pathway.

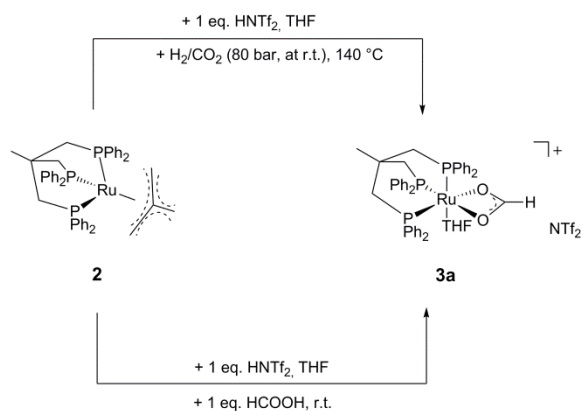
The sharp singlet at 43.3 ppm in the  $^{31}\text{P}\{^1\text{H}\}$ -NMR spectrum was correlated with a broad hydride signal at -8.7 ppm in the  $^1\text{H}$ -NMR spectrum by  $[\text{H}, ^{31}\text{P}]\text{-HMBC-NMR}$ . Comparison with literature data and analysis of the mixture by ESI-MS allowed unambiguous assignment to the dimeric complex  $[\text{Ru}_2(\mu\text{-H})_2(\text{Triphos})_2]$  (**6**), which formed in about 2 %. <sup>29</sup> Using isolated **6** in the CO<sub>2</sub> hydrogenation reaction under standard conditions showed no formation of methanol, revealing formation of **6** as a second major deactivation pathway.

The small sharp singlet at 36.7 ppm in the  $^{31}\text{P}\{^1\text{H}\}$ -NMR spectrum was assigned to  $[\text{Ru}_2(\text{Cl})_3(\text{Triphos})_2]^+$  (**7**) by comparison with literature data and analysis of the mixture by ESI-MS (6 % according to the integral ratios in the  $^{31}\text{P}\{^1\text{H}\}$ -NMR spectrum). <sup>34</sup> A CO<sub>2</sub> hydrogenation reaction under standard conditions using the  $[(\text{Triphos})\text{Ru}(\text{TMM})]$  (**2**) precursor but with the addition of 1-butyl-3-methylimidazolium chloride (3 eq.) gave only a TON of 1 after 24 hours. The  $^{31}\text{P}\{^1\text{H}\}$ -NMR spectrum of the solution showed the formation of **7**, **5** and  $[(\text{Triphos})\text{RuH}(\text{CO})\text{Cl}]$  (**18**) demonstrating that Ru-Triphos complexes bearing chloro ligands are again inactive in this transformation. <sup>35</sup>

The main species accounting for over 85 % of the total signal intensity in the  $^{31}\text{P}\{^1\text{H}\}$ -NMR gave rise to a broad singlet at 44.2 ppm, indicating fluxional behaviour at room temperature. Low-temperature NMR at 233 K resulted in splitting into a doublet (46.3 ppm, 2P,  $J = 42.5 \text{ Hz}$ ) and triplet (43.9 ppm, 1P,  $J = 42.5 \text{ Hz}$ ). A  $[\text{H}, ^{31}\text{P}]\text{-HMBC-NMR}$  experiment revealed a coupling of this signals to a proton signal at 8.7 ppm (bs), which is well in the range of ruthenium coordinated formate. <sup>36-38</sup> A  $[\text{H}, ^{13}\text{C}]\text{-HMBC-NMR}$  experiment showed the coupling of that proton signal to a singlet at 178.8 ppm in the  $^{13}\text{C}$ -NMR, further corroborating the formation of a formate-complex. <sup>23, 39, 40</sup> No hydride signals corresponding to this species were detected in the respective correlation NMR spectra.

The same formate complex could be generated independently by adding one equivalent of  $\text{HNTf}_2$  to complex **2** in  $d_8\text{-THF}$ , followed by the addition of one equivalent of  $\text{HCO}_2\text{H}$  at room temperature. NMR analysis of the crude reaction mixture at room temperature and 233 K showed the identical set of signals in the  $^{31}\text{P}\{^1\text{H}\}$ -NMR in about 80 % of the total intensity together with a second, yet unidentified phosphor containing species (singlet at 59 ppm, ca 20 % of total intensity), as well as in the  $^1\text{H}$ -NMR spectra (see ESI). FT-IR analysis of this solution at room temperature showed a  $\nu_{\text{CO}}$  stretching mode at  $1543 \text{ cm}^{-1}$ , a typical value for  $\eta^2$ -coordinated formate. <sup>37-40</sup> Based on these data and on basis of literature precedence, <sup>37</sup> we assign the structure of this complex as  $[(\text{Triphos})\text{Ru}(\eta^2\text{-O}_2\text{CH})(\text{THF})]^+$  (**3a**), where the weakly bound solvent molecule THF accounts for the fluxionality at room temperature (Scheme 3).

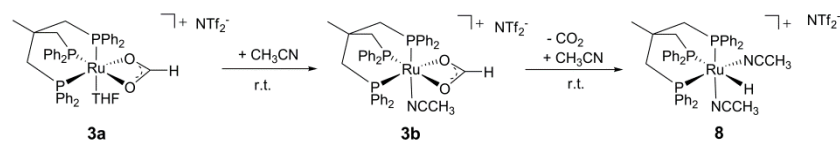
This interpretation is supported by the formation of a non-fluxional formate complex upon addition of 0.1 mL acetonitrile to the



**Scheme 3** Formation of the catalytically active formate complex **3a** from catalyst precursor **2** in presence of 1 eq.  $\text{HNTf}_2$  and  $\text{H}_2/\text{CO}_2$  under reaction conditions (upper pathway) and by addition of 1 eq.  $\text{HNTf}_2$  and 1 eq.  $\text{HCO}_2\text{H}$  in THF.

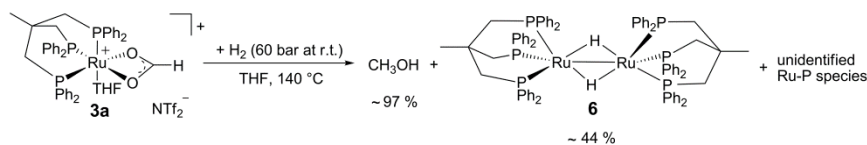
freshly prepared solution of **3a** in 0.5 mL THF at room temperature (d, 42.8 ppm, 2P; t, 29.6 ppm, 1P,  $J = 42.2 \text{ Hz}$ ; see ESI for details). FT-IR analysis of this solution at room temperature again showed a  $\nu_{\text{CO}}$  stretching mode at  $1544 \text{ cm}^{-1}$ , consistent with the structure  $[(\text{Triphos})\text{Ru}(\eta^2\text{-O}_2\text{CH})(\text{MeCN})]^+$  (**3b**). Interestingly, the signals of **3b** decreased over a period of 5 hours at room temperature at the expense of a new set of doublet (47.6 ppm, 2P,  $J = 20.6 \text{ Hz}$ ) and triplet (5.5 ppm, 1P,  $J = 20.6 \text{ Hz}$ ). In parallel, the formate signal at 8.7 ppm disappeared with concomitant formation of an upfield hydride signal (dt, -5.5 ppm,  $J = 105.0 \text{ Hz}$ ,  $J = 19.3 \text{ Hz}$ ) in the  $^1\text{H}$ -NMR. These NMR-data are consistent with the decarboxylation of **3b** to give the literature known complex  $[(\text{Triphos})\text{Ru}(\text{H})(\text{MeCN})_2]^+$  (**8**) (Scheme 4). <sup>41</sup> Consequently, the formation of the formate complex **3** from **2** in presence of  $\text{HNTf}_2$  under CO<sub>2</sub> and hydrogen pressure is most plausibly explained *via* reversible CO<sub>2</sub>-insertion into the analogous solvent-coordinated cationic Ru-hydride complex as intermediate.

Ruthenium-formate complexes are well known to be intermediates in the CO<sub>2</sub> hydrogenation to formic acid. <sup>42-44</sup> In order to probe whether the formate complex **3** is a kinetically competent intermediate in the hydrogenation of CO<sub>2</sub> to methanol, a solution of **3a** was prepared from **2**/ $\text{HNTf}_2$  (1:1) and  $\text{HCO}_2\text{H}$  in  $d_8\text{-THF}$ , pressurised only with 60 bar  $\text{H}_2$ , and heated to  $140^\circ\text{C}$  in an external oil bath in a high-pressure NMR tube for 40 minutes (Scheme 5). Indeed, this led to nearly quantitative conversion (ca. 97 %) of the coordinated formate to methanol based on  $^1\text{H}$ -NMR analysis (see ESI). In the corresponding  $^{31}\text{P}$ -NMR spectra the formation of  $[\text{Ru}_2(\mu\text{-H})_2(\text{Triphos})_2]$  (**6**) in about 44 % was observed. Furthermore, *in situ* high pressure NMR studies using complex **2** directly under turnover conditions (**2**/ $\text{HNTf}_2$  (1:1),  $d_8\text{-THF}$ ,  $T = 80^\circ\text{C}$ ,  $p(\text{H}_2) = 60 \text{ bar}$ ,  $p(\text{CO}_2) = 20 \text{ bar}$ ) revealed that complex **3a** was formed right after pressurisation and



**Scheme 4** Formation of the acetonitrile formate complex **3b** from **3a** by addition of MeCN to a solution of **3a** in THF and decarboxylation of **3b** to hydride complex **8** at room temperature.





**Scheme 5** Methanol is formed with high yield by hydrogenation of complex **3a**.

(**4**) with S being a free coordination site or weakly bound solvent molecule.<sup>46</sup> The formation of dimeric or trimeric species [(Triphos)Ru(μ-OAc)]<sub>x</sub>(NTf<sub>2</sub>)<sub>x</sub> could be excluded by using two structurally different Triphos derivatives and stirring an equimolar (12.5 μmol) mixture of [(Triphos)Ru(η<sup>2</sup>-OAc)Cl] (**9**) and [(Triphos-Anisyl)Ru(η<sup>2</sup>-OAc)Cl] (**10**) (Triphos-

remained the major detectable phosphorus containing species present in solution throughout the reaction. No hydride signals that could be related to an active species were observed in the <sup>1</sup>H-NMR spectra (see ESI). These data indicate that the presumed cationic hydride intermediate is too short-lived to be observed on the NMR-time-scale,<sup>37</sup> but is converted to the observable formate complex [(Triphos)Ru(η<sup>2</sup>-O<sub>2</sub>CH)(THF)]<sup>+</sup> **3a** as the resting state by rapid and reversible CO<sub>2</sub> insertion into the metal-hydride bond under turnover conditions.<sup>38, 42-44</sup>

Identification of the formate complex **3** as the active intermediate suggests that the major role of the acid additive in the catalytic system **2**/HNTf<sub>2</sub> is the generation of cationic species as the active site upon reductive removal of the TMM-ligand. In order to probe this assumption, we decided to start from an isolated cationic complex as precursor. After numerous unsuccessful attempts to isolate complex **3** in stable form as solid, we turned our efforts towards the analogous cationic acetate complex. Stirring [(Triphos)Ru(η<sup>2</sup>-OAc)Cl] (**9**)<sup>45</sup> together with one equivalent AgNTf<sub>2</sub> for 3 h at 60 °C in THF led to the precipitation of AgCl. The <sup>31</sup>P{<sup>1</sup>H}-NMR spectrum showed the selective formation of only one sharp singlet at 44.0 ppm, indicating the formation of a symmetrical complex species. After filtration of the yellow solution over silica and removal of the solvent *in vacuo* a yellow powder was obtained. Characterisation of the material by <sup>1</sup>H-, <sup>13</sup>C- and <sup>19</sup>F-NMR, FT-IR and by ESI-HRMS revealed the presence of the cationic [(Triphos)Ru(η<sup>2</sup>-OAc)]<sup>+</sup> fragment (see ESI). Crystallisation from dichloromethane layered with pentane gave yellow single crystals of complex **4a** where the open coordination site was saturated with H<sub>2</sub>O from adventitious traces of water (Fig. 2). Thus, the acetate complex in solution can be formulated as [(Triphos)Ru(η<sup>2</sup>-OAc)(S)][NTf<sub>2</sub>]

Anisyl = 1,1,1-tris{bis(4-methoxyphenyl)phosphinemethyl}ethane together with AgNTf<sub>2</sub> (30 μmol) in toluene (1.5 mL) at 60 °C for 5 hours. The toluene was removed *in vacuo*, the residue dissolved in *d*<sub>2</sub>-DCM (0.5 mL), and the mixture analysed by NMR. The <sup>31</sup>P{<sup>1</sup>H}-NMR spectrum at room temperature showed two singlets at 43.5 and 45.3 ppm in a ratio of nearly 1:1 related to [(Triphos)Ru(η<sup>2</sup>-OAc)(S)]NTf<sub>2</sub> (**4**) and [(Triphos-Anisyl)Ru(η<sup>2</sup>-OAc)(S)]NTf<sub>2</sub> (**11**), respectively. The absence of further signals due to mixed complexes (e.g. [Ru<sub>2</sub>(Triphos)(Triphos-Anisyl)(μ-OAc)<sub>2</sub>](NTf<sub>2</sub>)<sub>2</sub>) supports the monomeric structure of **4** in solution.<sup>47</sup>

The reactivity of the acetate complex **4** under CO<sub>2</sub> (20 bar at r.t.) and H<sub>2</sub> (60 bar at r.t.) pressure was investigated in a HP-NMR experiment (see ESI). After 1.5 hours at 80 °C and 1 hour at 140 °C, ca. 60 % (<sup>31</sup>P{<sup>1</sup>H}-NMR) of **4** was converted to the formate complex **3a** and ethanol from acetate hydrogenation was detected by <sup>1</sup>H-NMR in the reaction mixture. Methanol was indeed observed in the solution with a TON of 5, confirming that cationic complex **4** was operating as molecularly defined direct precursor for the catalytic cycle for CO<sub>2</sub> hydrogenation without the need of any acid additive.

### Mechanistic pathways on basis of DFT calculations

In summary, the experimental results described above clearly demonstrate that the Ru-Triphos framework is able to act as molecular single-site catalyst for the hydrogenation of CO<sub>2</sub> to methanol. All observations are in accordance with a stepwise reduction of CO<sub>2</sub> to methanol *via* the formate anion in the coordination sphere of a homogeneous cationic organometallic complex. Complex **3**, which is accessible from different precursors in the presence or absence of acid co-catalysts, represents the resting state under turnover conditions. Consequently, spectroscopic insight into the subsequent reduction steps cannot be obtained directly. We therefore used DFT calculations to explore possible reaction pathways for this multi-step transformation. Based on our previous investigations on the Ruthenium-Triphos system and on recent work by other groups on catalytic hydrogenation of CO<sub>2</sub> or methanol reforming, a plausible basic catalytic cycle that reduces carbon dioxide stepwise through the formic acid and formaldehyde stage to methanol *via* the key intermediates **I**, **V**, **IX**, **XVIII** can be formulated as shown in Scheme 6.<sup>21, 23, 28, 30, 37, 48-51</sup>

Starting from a cationic Ruthenium-hydride complex **I**, the migratory insertion of CO<sub>2</sub> results in the formation of the spectroscopically observed Ruthenium-formate species **V**. Reaction with one equivalent of hydrogen leads to reduction beyond the formic acid stage to give the respective Ruthenium-hydroxymethanolate species **IX**, which is then transformed to the Ruthenium-methanolate complex **XVIII** *via* intermediate formation of formaldehyde and consumption of a second

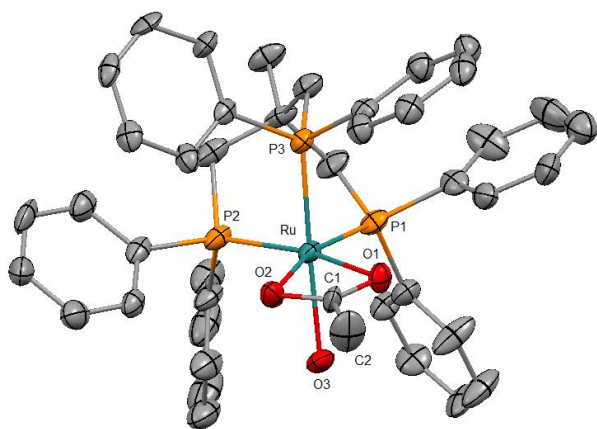
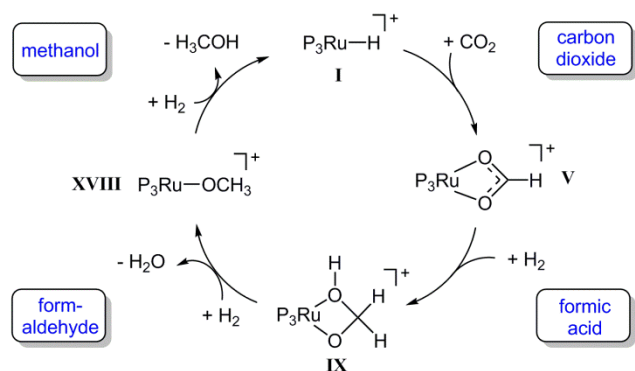


**Fig. 2** Molecular structure of the cation **4a** (S = H<sub>2</sub>O) in the solid state as derived from single crystal X-ray diffraction (hydrogen atoms are omitted for clarity). Some selected bond lengths (Å): Ru-P1 = 2.245(9); Ru-P2 = 2.255(3); Ru-P3 = 2.253(0); Ru-O1 = 2.171(2); Ru-O2 = 2.208(6); Ru-O3 = 2.204(7).



**Scheme 6** Basic catalytic cycle for the transformation of CO<sub>2</sub> to methanol at the Ru-Triphos fragment *via* the formic acid and formaldehyde stage through the key intermediates **I**, **V**, **IX**, **XVIII**. P<sub>3</sub>Ru denotes the Triphos-Ru(+II) fragment comprising additional ligands to fill the coordination sphere as discussed in the detailed analysis.

equivalent of hydrogen.<sup>30, 50, 51</sup> In the last step, hydrogenolysis of the Ru-OMe unit requires the third equivalent of H<sub>2</sub> to liberate the product and closes the cycle by restoring the Ruthenium-hydride complex **I**. A plausible structure for complex **I** as starting point of the calculations is the cationic species [(Triphos)Ru(H)(H<sub>2</sub>)(THF)]<sup>+</sup> that is, for example, most likely to be formed from complex **4** upon hydrogenative removal of the acetate ligand as the initiating step.<sup>28</sup> The individual steps of the cycle shown in Scheme 6 were therefore analysed in detail from this starting point, whereby the reduction steps are composed of hydride migration/protonolysis events. For clarity we constrain the discussion here to the energetically most favourable pathways and some particularly relevant alternatives and refer the reader to the SI for additional information.

*Formation of hydroxymethanolate via formic acid (I – IX, Figure 3):* The insertion of CO<sub>2</sub> into metal-hydride bonds and subsequent hydrogenolysis of the metal-formate units has been subject of numerous experimental and theoretical studies in the context of formic acid production. The closest related example to the Triphos-system are Ru(II)-catalysts bearing three monodentate phosphine ligands whose high efficiency for formic acid production was rationalised in a comprehensive theoretical study by the group of Sakaki.<sup>48</sup> An analogous route was therefore investigated for the initial step of the current system (Figure 3).

In the starting complex **I** either the THF molecule or the H<sub>2</sub> molecule is replaced by CO<sub>2</sub> generating complexes **II** and **IIa**, respectively. Both compounds are endergonic with respect to the reference point **I** by 8 and 10.2 kcal/mol. The classical hydride centre in **II** can subsequently be transferred to the carbon atom of CO<sub>2</sub> passing transition state **TSII-III**. The barrier is appreciably low (11.7 kcal/mol) placing the **TSII-III** at 21.2 kcal/mol on the

hyper surface. Rotation of the formate species in **III** about the Ru-O and the O-C-bond generates complex **IV** (3.3 kcal/mol), which is significantly more stable than **III**.<sup>43, 48</sup> The barrier for the dissociation of H<sub>2</sub> from **IV** is very low (4.2 kcal/mol) and the exchange of H<sub>2</sub> in **IV** by solvent generates the stable ruthenium formate complex **V** (-3.2 kcal/mol), which is also the experimentally observed resting state complex **3a**.

In accord with the work by Sakaki, the proton transfer to the carbonyl C=O bond in the six-membered transition state is also energetically favourable in the Ru-Triphos system.<sup>48</sup> The change of coordination mode of the formate species in **V** from bidentate to monodentate with subsequent coordination of H<sub>2</sub> at the vacant coordination site forms **VI**. The coordinated H<sub>2</sub> molecule is cleaved heterolytically *via* **TSVI-VII** with a very small barrier of 1.7 kcal/mol to **VII** (12.5 kcal/mol). At this point of the cycle the generation of formic acid is completed and the Ru-H unit for further reduction is regenerated.

In contrast to hydrogenation of CO<sub>2</sub> to formic acid, far less is known about the reduction beyond the formate level. Only most recently, Ruthenium and Iridium catalysts have been reported to facilitate this reaction step *via* unprecedented catalytic pathways.<sup>30, 50, 52, 53</sup> In the Ru-Triphos system, the hydride transfer on to the coordinated formic acid was found to be energetically feasible only after the solvent in **VII** is replaced by H<sub>2</sub> generating complex **VIII**. The exchange of solvent by H<sub>2</sub> is almost thermoneutral placing **VIII** at an energy of 14.3 kcal/mol. The hydride transfer in **VIII** to the carbon atom of formic acid has a barrier of 15.5 kcal/mol, placing **TSVIII-IX** at 29.8 kcal/mol on the hyper surface. This energetically well accessible reaction step forms the Ruthenium-hydroxymethanolate species (**IX**) which is the crucial intermediate for the unique performance of the Ru-Triphos system in the hydrogenation of CO<sub>2</sub> beyond the formic acid stage. Three other energetically less favoured reaction pathways for the formation of hydroxymethanolate from CO<sub>2</sub>, including outer sphere attack of CO<sub>2</sub>, were calculated and are shown in the ESI. The next key step is the cleavage of the carbon-

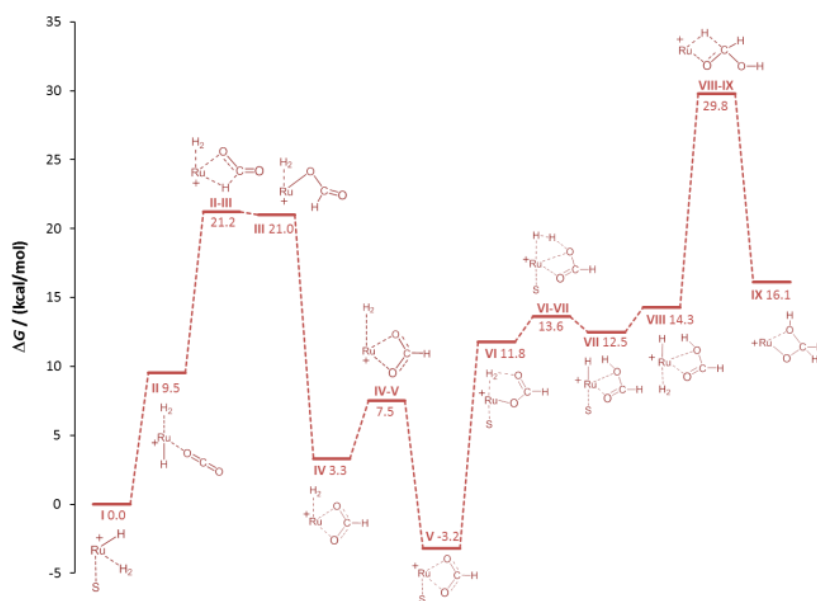


**Fig. 3** Initial steps of the DFT calculated reaction pathways for the hydrogenation of CO<sub>2</sub> to methanol at the cationic Ru-Triphos centre, starting from complex **I** (S = THF) as the active species. The Triphos ligand is omitted for clarity.

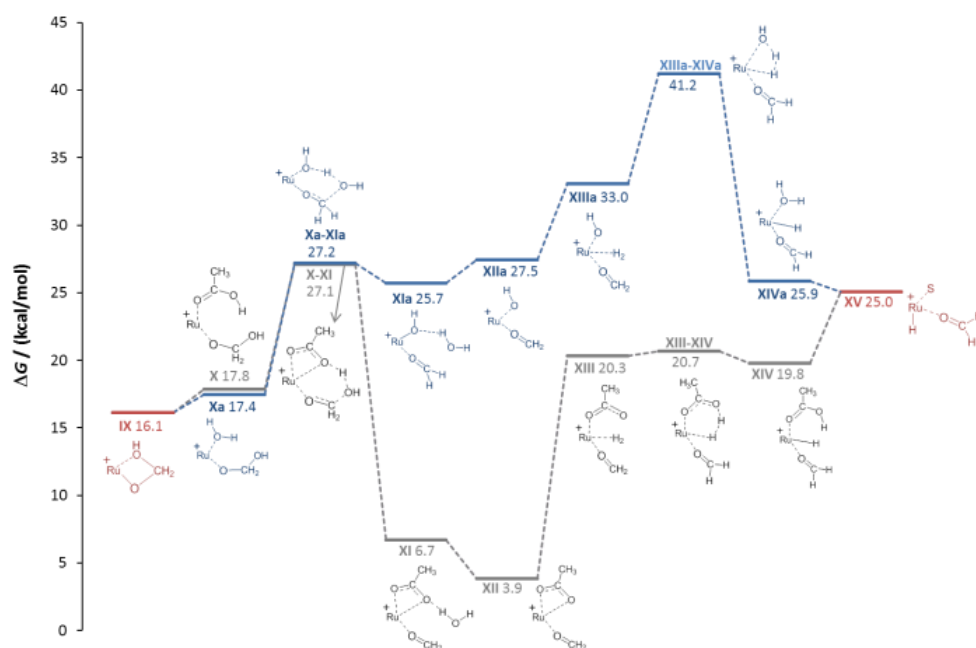


**Fig. 4** Calculated reaction pathways generating formaldehyde complex **XV** via medium-assisted proton transfer (acetate: grey; water: blue). The Triphos ligand is omitted for clarity, S = THF.

oxygen bond leading to formaldehyde on the path to methanol.

*Cleavage of the C-O bond and generation of formaldehyde (IX – XV; Figure 4):* The conversion between free methanediol and formaldehyde has been largely explored.<sup>50</sup> In the coordination sphere of **IX**, the protonolysis of the Ru-O is again required to initiate this process. Firstly, we considered transfer of protons generated from the acidic Ru-H<sub>2</sub> units under turnover conditions via the reaction medium (Figure 4). A low energy pathway (grey profile) was calculated if acetic acid was used as model for carboxylate units as proton shuttles in the presence of catalyst precursors **4** (acetate) or **2** (formate) according to the in situ NMR studies. After de-coordination of the hydroxy group in the hydroxymethanolate species **IX**, a molecule of acetic acid coordinates *via* the carbonyl oxygen atom forming **X** in a practically a thermoneutral event. The acetic acid then protonates the hydroxy group of the hydroxymethanolate (**TSX-XI**, 27.1 kcal/mol), with a barrier of 9.3 kcal/mol. Water is loosely coordinated after the reaction (**XI**) and cleaved off generating **XII**. Dissociation of one of the acetate oxygen atoms of **XII**, changing the acetate coordination from bi- to monodentate, and association of H<sub>2</sub> generates **XIII**, which is placed at a height of 20.3 kcal/mol. The subsequent heterolytic cleavage of H<sub>2</sub> under regeneration of acetic acid is practically barrierless (0.4 kcal/mol) and product **XIV** is only marginally more stable than the reactant. Dissociation of acetic acid and association of solvent generates **XV**. An analogous path using water, which is formed stoichiometrically in the overall hydrogenation sequence, as the proton shuttle gave a significantly higher barrier of 41.2 kcal/mol (**XIIIa-XIVa**, blue profile). In addition to the external proton transfer, direct protonolysis within the coordination sphere was also investigated (see ESI).

In essence, the C-O bond cleavage can be achieved from the hydroxymethanolate intermediate **IX** through pathways involving

medium-assisted proton transfer or intramolecular proton transfer within the coordination sphere of the Ru-centre. The lowest energy pathway (ca. 28 kcal/mol) from the presently investigated alternatives is provided by external proton transfer using carboxylates as proton shuttle. The intramolecular pathways result in significantly higher barriers (ca. 40 kcal/mol), but still provide general viable alternatives that are also in line with the experimental results described below.

*Hydrogenation of formaldehyde to methanol (XV-I'; Figure 5):* Once the formaldehyde level is reached in complex **XV** the solvent

can be replaced again by H<sub>2</sub> to arrive at **XVI**. The subsequent migratory transfer of the classical hydride (**TSXVI-XVII**) is almost barrierless with 0.7 kcal/mol and leads to the methanolate complex **XVII** that is stabilised by an agostic C-H-Ru interaction. Association of a solvent molecule opens the agostic bond to give **XVIII**. The intramolecular proton transfer from the coordinated H<sub>2</sub>-molecule through the “σ-bond metathesis-like”<sup>54,55</sup> four-membered transition state **TSXVIII-XXIV** has an energy barrier of 31.5 kcal/mol. Finally, the reaction product methanol dissociates from the corresponding complex **XXIV** and for completeness we calculated the barrier **TSXXIV-I'** for H<sub>2</sub> association, which is below 10 kcal/mol indicating this process to be facile. It should be noted that **I'** lies 14.1 kcal/mol above the reference point, indicating the overall reaction to be endergonic under the boundary conditions of the calculation model. The inclusion of solvent effects, however, predicts the reaction to be exergonic, in accordance with the experimental observation and standard state thermodynamics (see ESI for details).

Similar to the protonolysis of the hydroxymethanolate complex, carboxylate-assisted proton transfer provides an alternative low energy pathway. Substitution of the hydrogen molecule in **XVIII** by acetic acid is energetically favourable to give **XX** and subsequent protonation of the methanolate oxygen atom *via* **TSXX-XXI** has no significant barrier and results in the acetate-methanol complex **XXI** (-2.2 kcal/mol). Hydrogen addition (**XXII**) and carboxylate assisted heterolytic cleavage of H<sub>2</sub> to regenerate acetic acid (**XXIII**) can occur through a six-membered transition state, rendering this more facile than the direct heterolytic cleavage of the Ru-methanolate unit. Dissociation of acetic acid leads to **XXIV** at which point the two pathways merge again.

Overall, the results of the DFT calculations demonstrate the possibility of a stepwise reduction of CO<sub>2</sub> to methanol in the

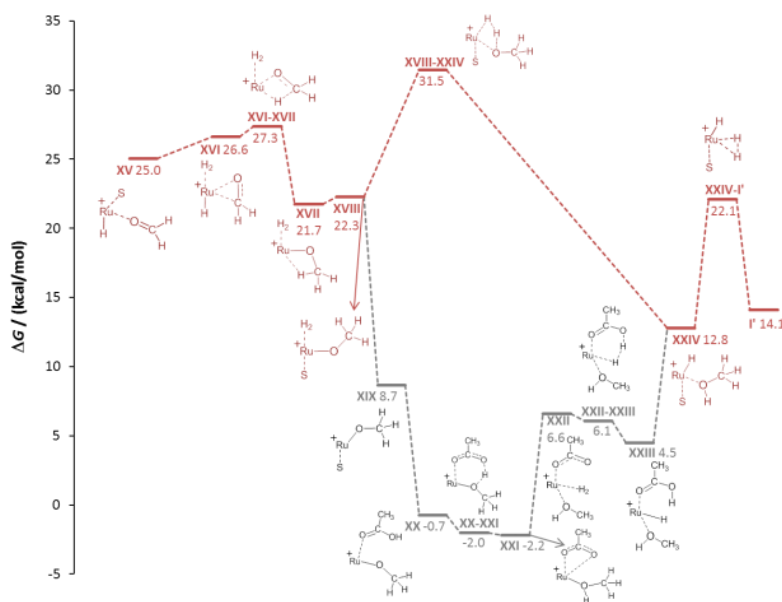


**Fig. 5** Calculated reaction pathways for the hydrogenation of formaldehyde generating methanol *via* intramolecular proton transfer (red) and carboxylate assisted proton transfer (acetic acid: grey). The Triphos ligand is omitted for clarity, S = THF.

coordination sphere of a single Ru-Triphos centre. The individual reduction steps occur by migratory transfer of classical Ru-hydride ligands, exhibiting low to moderate barriers in all cases. The protonolysis steps of the resulting Ru-O bonds can occur intramolecularly *via* heterolytic cleavage of coordinated H<sub>2</sub> molecules. External proton transfer assisted by carboxylate groups present under turnover conditions may lower the corresponding barriers significantly.

## Parameter variation and catalyst recycling in a biphasic system

After demonstrating the principle possibility for the catalytic hydrogenation of CO<sub>2</sub> to methanol in the absence of an alcohol additive, the performance of the Ru-Triphos precursor systems **2** and **4** was evaluated further by systematic variation of key reaction parameters and the results were corroborated for consistency with the mechanistic proposal (Table 1).

Firstly, the catalyst systems **2** and **4** were compared under a standard set of reaction conditions (*V*(THF) = 2.08 mL, *c*(Ru) = 12 mmol/L, *p*(CO<sub>2</sub>) = 20 bar at r.t., *p*(H<sub>2</sub>) = 60 bar at r.t., = 140°C, *t* = 24 h). Using **4** as catalyst precursor for the CO<sub>2</sub> hydrogenation in THF gave a TON (turnover number = mmol MeOH/mmol catalyst) of 165 in the absence of any additives (Table 1, entry 3). Using an additional 0.5 eq. HNTf<sub>2</sub> did not show an increased TON (Table 1, entry 4). In contrast precursor **2** showed only a very poor performance in the absence of the acid additive (Table 1, entry 2). However, a TON of 228 was found when conducting a CO<sub>2</sub> hydrogenation reaction with catalyst **2** and 1 eq. of HNTf<sub>2</sub> (Table 1, entry 1). The need for an acid additive in the case of precursor **2** is consistent with the formation of the cationic species [(Triphos)Ru(H)(H<sub>2</sub>)(S)]<sup>+</sup>, which is the catalytically active species **I** used as starting point in the calculated catalytic cycle.

The lower TON obtained when using the acetate complex **4** instead of **2**/HNTf<sub>2</sub> (1:1) under otherwise identical conditions can be explained by the less efficient initiation with **4** due to more difficult hydrogenation of the acetate groups to form the common intermediate **3a** (*vide supra*). This distinct reactivity is also reflected in catalytic experiments for the hydrogenation of the corresponding free acids: Using **2** together with 1 eq. HNTf<sub>2</sub>, 100 equivalents of formic acid could be fully converted to methanol at a hydrogen pressure of 60 bar (at r.t.) and a reaction temperature of 140 °C within 24 hours, whereas a reaction temperature of 180 °C was necessary for the full conversion acetic acid to ethanol (*c*(Ru) = 12.5 mmol/L, 2.0 mL THF). The efficient hydrogenation of formic acid under these conditions is in accordance with

the proposed catalytic cycle shown in Scheme 6. To complete the picture, the hydrogenation of 100 equivalents of paraformaldehyde was also assessed and full conversion was indeed achieved with the same catalytic system (*c*(Ru) = 12.5 mmol/L, 2.0 mL THF, 0.2 mL H<sub>2</sub>O, 60 bar H<sub>2</sub> at r.t., 140 °C, 24 h). Again, formation of formate complex **3a** was observed in <sup>31</sup>P{<sup>1</sup>H}-NMR, indicating full reversibility of the catalytic cycle.

**Table 1** Hydrogenation of carbon dioxide to methanol in the absence of alcohol additive.<sup>[a]</sup>

Entry	Cat	Acid (eq)	<i>T</i> [°C]	<i>p</i> <sub>H<sub>2</sub></sub> / <i>p</i> <sub>CO<sub>2</sub></sub> <sup>[b]</sup> [bar/bar]	TON <sup>[c]</sup>
1	<b>2</b>	HNTf <sub>2</sub> (1.0)	140	20/60	228
2	<b>2</b>	-	140	20/60	8
3	<b>4</b>	-	140	20/60	165
4	<b>4</b>	HNTf <sub>2</sub> (0.5)	140	20/60	156
5	<b>2</b>	HNTf <sub>2</sub> (1.5)	140	20/60	196
6	<b>2</b>	HNTf <sub>2</sub> (2.0)	140	20/60	181
7	<b>2</b>	<i>p</i> -TsOH (1.0)	140	20/60	135
8	<b>2</b>	HNTf <sub>2</sub> (1.0)	120	20/60	169
9	<b>2</b>	HNTf <sub>2</sub> (1.0)	100	20/60	67
10	<b>2</b>	HNTf <sub>2</sub> (1.0)	80	20/60	24
11	<b>2</b>	HNTf <sub>2</sub> (1.0)	140	10/30	78
12	<b>2</b>	HNTf <sub>2</sub> (1.0)	140	30/90	367
13	<b>2</b>	HNTf <sub>2</sub> (1.0)	140	20/80	301
14	<b>2</b>	HNTf <sub>2</sub> (1.0)	140	20/100	348
15 <sup>[d]</sup>	<b>2</b>	HNTf <sub>2</sub> (1.0)	140	20/60	335
16 <sup>[e]</sup>	<b>2</b>	HNTf <sub>2</sub> (1.0)	140	20/60	442
17 <sup>[d]</sup>	<b>12</b>	HNTf <sub>2</sub> (1.0)	140	20/60	256

[a] Reaction conditions: 25 μmol [Ru], 2.08 mL THF, 24 h; [b] = at room temperature; [c] TON = mmol MeOH/mmol catalyst; [d] 12.5 μmol [Ru];

[e] 6.3 μmol [Ru].

The lack of activity with catalyst **2** in absence of acid can be directly corroborated with the formation of the neutral complex [(Triphos)Ru(H)<sub>2</sub>CO] (**12**), which was observed as the almost exclusive species present in solution by <sup>31</sup>P{<sup>1</sup>H}-NMR



spectroscopy under these conditions (see ESI).<sup>28</sup> The protonation of this complex with strong protic acids was shown by Zanobini et al. to lead to the formation of the complex [(Triphos)Ru(CO)(H)(H<sub>2</sub>)]<sup>+</sup> (**13**), a cationic structure closely resembling the active hydride species **I** inferred above.<sup>56</sup> Using the isolated complex **12** together with 1 equivalent of HNTf<sub>2</sub> in THF resulted indeed in an active catalyst for the CO<sub>2</sub> hydrogenation reaction yielding a TON of 256 after 24 h (Table 1, entry 17) which is about 76 % of the TON obtained using the catalyst **2**/HNTf<sub>2</sub> under identical conditions (Table 1, entry 15). Again, formation of the formate intermediate **3a** was observed when the solution was analysed by <sup>31</sup>P{<sup>1</sup>H}-NMR (see ESI).

Variation of the amount of HNTf<sub>2</sub> added to complex **2** revealed a maximum of the observed TON at the 1:1 ratio (Table 1, entries 5-6) corresponding to the stoichiometric ratio required for the reductive removal of the TMM-ligand leading to **I**. Using **2** together with 1 eq. *p*-TsOH instead of HNTf<sub>2</sub> gave a lower TON of 135 (Table 1, entry 7) under otherwise identical conditions. NMR-analysis of the reaction solution after 1 h reaction time showed the formation of the formate species **3a** as major component in solution in both cases (see ESI). However, [(Triphos)Ru(*p*-TsO)<sub>2</sub>] (**14**) was present also in about 15 % as indicated by a broad singlet at 38.7 ppm in the <sup>31</sup>P{<sup>1</sup>H}-NMR spectrum measured at room temperature, which split up into a triplet ( $\delta$  = 42.0 ppm,  $J$  = 47.5 Hz) and doublet ( $\delta$  = 36.1 ppm,  $J$  = 47.5 Hz) when measured at 233 K in *d*<sub>8</sub>-THF. This assignment was supported by mass spectrometry (FAB) and independent generation of **14** by addition of 2 equivalents of *p*-TsOH to **2** in THF at room temperature. Thus, the presence of even weakly-coordinating anions in the reaction mixture hampers the formation of the formate species **3a**, explaining the preferred choice of HNTf<sub>2</sub> as acid additive.

Identifying the system **2**/HNTf<sub>2</sub> (1:1) as the most practical and effective catalyst precursor so far, the influence of some key reaction parameters on the TON after 24 hours reaction time was assessed. Lowering the catalyst concentration together with the acid concentration from 12 μmol/mL to 6 μmol/mL and further to 3 μmol/mL resulted in a significant increase in TON from 228 to 335 and 442, respectively (Table 1, entries 1 and 15-16). Although final conclusions have to await a detailed kinetic analysis, the formation of the dimeric complex **6** as part of the deactivation mechanism is in line with this trend. Decreasing the reaction temperature to 120 °C, 100 °C and 80 °C resulted in reduced TONs of 169, 67 and 24 (Table 1, entries 8-10). Variation of the total pressure while maintaining the stoichiometric ratio of  $p(\text{CO}_2)/p(\text{H}_2) = 1/3$  from 40 bar to 80 bar and 120 bar resulted in an increase of the obtained TONs from 78 to 228 and 367 (Table 1, entries 1 and 11-12). Using an excess of H<sub>2</sub> (20 bar CO<sub>2</sub> + 80 bar or 100 bar H<sub>2</sub>) resulted in largely increased TONs of 301 and 348, respectively (Table 1, entries 16-17). In the latter case about 40 % of the totally available carbon feedstock CO<sub>2</sub> was converted to methanol, as calculated from the amount of MeOH formed (8.7 mmol) and the amount of CO<sub>2</sub> initially charged (22.1 mmol, determined by weight).

A conversion/time profile of the CO<sub>2</sub> hydrogenation to methanol in THF using **2**/HNTf<sub>2</sub> (1:1, 12.5 μmol; otherwise standard conditions) was mapped out by termination of batch

reactions after different reaction times (Figure 6). The reaction started without any pronounced induction period reaching a TON of 70 already after 1 hour. This corresponds to an initial turnover frequency (TOF) of 70 h<sup>-1</sup> that is well in the range of the activity of the active sites in the state-of-the-art heterogeneous Cu/ZnO-based catalysts.<sup>18</sup> Methanol formation continued smoothly to reach a TON of 258 after 16 hours. At this point the pressure in the reactor vessel had dropped from initially 120 bars to 72 bars due to the consumption of the reactive gases. Therefore, a reaction was conducted for 32 h where the reactor was re-pressurised to the initial pressure with  $p(\text{CO}_2)/p(\text{H}_2) = 1/3$  after 16 hours leading to TON of 478. Finally, a reaction was run for 48 hours with re-pressurisation to the initial pressure with  $p(\text{CO}_2)/p(\text{H}_2) = 1/3$  after 16 hours and again after 32 hours, yielding a total TON of 603. These experiments clearly indicate the high stability of the active catalyst resulting in a nearly linear increase of the TON under isobaric conditions. The absence of an induction period indicates that the presence of methanol is not enhancing the rate of catalysis under these conditions. This does not rule out the possibility that the reaction proceeds partly also via a cascade reaction involving methyl formate as intermediate once methanol has been formed, as catalyst **2** is able to promote the hydrogenation of alkyl formates to methanol.<sup>24</sup>

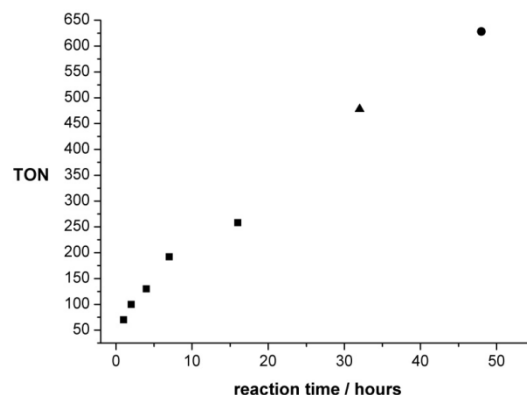


**Fig. 6** Conversion/time-profile of the hydrogenation of CO<sub>2</sub> to methanol using catalyst **2** (12.5 μmol catalyst **2**; 12.5 μmol HNTf<sub>2</sub>, 20 bar CO<sub>2</sub> + 60 bar H<sub>2</sub> at r.t.; 140 °C reaction temperature; 2.08 mL THF), as obtained from batch experiments terminated at the given reaction times. In the case of the reaction terminated after 32 h the autoclave was re-pressurised to the initial pressure with  $p(\text{CO}_2)/p(\text{H}_2) = 1/3$  after 16 h (▲). In the case of the reaction terminated after 48 h the autoclave was re-pressurised after 16 h and again after 32 h (●).

As all previous results are consistent with the cationic Ru-Triphos formate complex **3** as resting state in this process, we explored strategies for the recycling of the catalyst in active form. Considering the various options for the isolation of the product MeOH from the homogeneous catalyst, distillation seems an obvious possibility. However, the hydrogenation of CO<sub>2</sub> yields a stoichiometric amount of water, which is the least volatile component in the THF/MeOH/water product mixture. Thus, it would accumulate upon stripping of the MeOH product, ultimately becoming the limiting factor even if the catalyst would be thermally stable for recycling. Multiphase catalysis offers an alternative strategy, where the separation is based on differences in solubility rather than volatility. For the current process, an

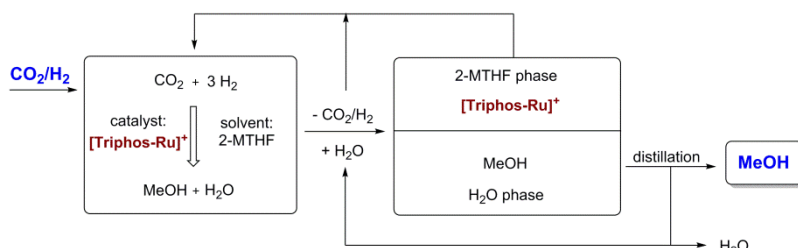


**Fig. 7** Aqueous biphasic system for recycling of the cationic Ru-Triphos catalyst in the organic 2-MTHF phase and removing the product MeOH in the aqueous phase for downstream processing.

aqueous biphasic system was envisaged, where the catalyst is retained and recycled in an organic phase, whereas the product is removed in an aqueous phase for downstream processing.<sup>57, 58</sup> Substitution of the solvent THF with 2-methyl tetrahydrofuran (2-MTHF) opens up the possibility for the realisation of such a two phasic reaction/separation system as 2-MTHF has a miscibility gap with water.<sup>27</sup> All material streams can be recycled internally in such a process scheme providing also the possibility for continuous-flow operation (Figure 7).

Assessing the partitioning of methanol in a 2-MTHF/water biphasic mixture showed that 80 % of 0.2 mL MeOH can be isolated from 1.0 mL of 2-MTHF using 1.0 mL water in a single extraction step. Application of 2-MTHF as solvent for the catalytic reaction under standard conditions ( $p(\text{CO}_2) = 20 \text{ bar}$  /  $p(\text{H}_2) = 60 \text{ bar}$  at r.t.,  $T = 140^\circ\text{C}$ ,  $V(\text{solvent}) = 2.08 \text{ mL}$ ) was also found to be possible without any problem for catalyst **2** (25  $\mu\text{mol}$  complex **2**,  $2/\text{HNTf}_2 = 1:1$ ), albeit with a somewhat lower TON of 186 after 24 h as compared to THF. To validate the combination of reaction and separation, a reaction with **2** (12.5  $\mu\text{mol}$  complex **2**,  $2/\text{HNTf}_2 = 1:1$ ) in 2-MTHF (2.0 mL) was terminated after 16 hours, the reaction mixture extracted by addition of 2.0 mL  $\text{H}_2\text{O}$ , and the orange catalyst/2-MTHF phase recycled to the autoclave after simple decantation. A small amount of fresh 2-MTHF (0.25 mL) was added to compensate for any loss of 2-MTHF with the product phase. The aqueous layers were analysed for MeOH content by quantitative  $^1\text{H-NMR}$  in  $d_6$ -acetone using mesitylene as standard, and only the concentration in the aqueous streams was used for the calculation of the apparent TON. As seen from Figure 8, the catalyst system

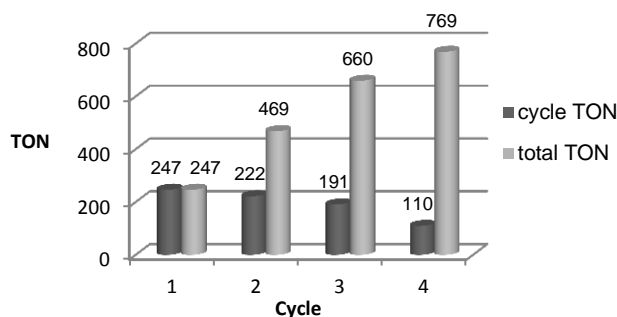


**Fig. 8** Recycling of catalyst system **2** (12.5  $\mu\text{mol}$  complex **2**,  $2/\text{HNTf}_2 = 1:1$ ) using MTHF (2.0 mL) as solvent and water (2.0 mL) as extracting agent in an aqueous biphasic system. Each cycle was run for 16 h (20 bar  $\text{CO}_2$  + 60 bar  $\text{H}_2$  at r.t.;  $140^\circ\text{C}$  reaction temperature). The TONs obtained per cycle are shown in dark grey, the total TONs summing up the cycles are shown in light grey.

**2**/HNTf<sub>2</sub> could be recycled three times, resulting in a total TON of 769 after 4 cycles. The TON per cycle was reduced significantly especially between cycle three and four, but still nearly 50 % of the initial productivity was retained in this non-optimised sequence.

## Conclusions

The results of this study demonstrate for the first time the hydrogenation of  $\text{CO}_2$  to methanol using a single organometallic catalyst in homogeneous solution without the need for an alcohol additive. The experimental and theoretical results are consistent with a mechanistic picture where this unprecedented transformation occurs at a cationic Triphos-Ru fragment as molecularly-defined active site. The cationic formate complex  $[(\text{Triphos})\text{Ru}(\eta^2\text{-O}_2\text{CH})(\text{S})]^+$  (**3**) ( $\text{S}$  = solvent) represents the resting state of the catalytic cycle under turnover conditions and can be obtained from various stable and readily available catalyst precursors. Through a series of hydride transfer and protonolysis steps, the  $\text{CO}_2$  reduction can pass through the formic acid and formaldehyde stage within the coordination sphere of a single ruthenium centre. The barriers for the proton transfer steps may be significantly lowered if assisted by the reaction medium. The active species shows a remarkable stability, with decarbonylation and dimerisation as potential deactivation mechanisms. Recycling of the catalyst is possible in the aqueous biphasic system 2-MTHF/water, opening the possibility for continuous-flow operation.

The Triphos-Ruthenium system is the very first homogeneous catalyst to enable this transformation. The facial coordination of the Triphos ligand imposes a favorable geometrical arrangement for the hydride transfer to carboxylate units in general (see ESI for a comparison of facial with meridional arrangement).<sup>28</sup> Furthermore, the heterolytic cleavage of hydrogen offers low-energy pathways for the protonolysis of Ru-O units under regeneration of the hydride ligand. Together with the high thermal stability of Triphos-Ruthenium complexes, these features seem to play an important role in the reduction of  $\text{CO}_2$  beyond the formate level with this catalyst. Further developments on the basis of the methodological approach of organometallic chemistry e.g. by systematic ligand variation based on the current mechanistic hypothesis are likely to produce even more active and stable systems. Already at this early stage of the development, turnover frequencies per Ru-centre are in the same range as for the active sites in traditional heterogeneous catalysts for methanol synthesis. The possibility to operate under multiphase conditions provides opportunities to overcome the limitations in productivity inherent to batch or repetitive batch operation. Therefore, we believe that the results of this study provide not only fundamental mechanistic insight into the activation and transformation of  $\text{CO}_2$  and  $\text{H}_2$  in organometallic chemistry, but also open promising targets for research at the interface of molecular and engineering sciences.

## Acknowledgements

This work was supported in part by the Cluster of Excellence

"Tailor-Made Fuels from Biomass", which is funded by the Excellence Initiative by the German Federal and State Governments to promote science and research at German universities and in part by the project SusChemSys. The project "Sustainable Chemical Synthesis (SusChemSys)" is co-financed by the European Regional Development Fund (ERDF) and the state of North Rhine-Westphalia, Germany, under the Operational Programme "Regional Competitiveness and Employment" 2007-2013. Generous allocation of computer time by the Computation and Communication Centre of RWTH Aachen University is gratefully acknowledged.

## References

1. M. Peters, B. Koehler, W. Kuckshinrichs, W. Leitner, P. Markewitz and T. E. Mueller, *ChemSusChem*, 2011, **4**, 1216-1240.
2. M. Cokoja, C. Bruckmeier, B. Rieger, W. A. Herrmann and F. E. Kühn, *Angew. Chem. Int. Ed.*, 2011, **50**, 8510-8537.
3. M. Aresta and A. Dibenedetto, *Dalton Trans.*, 2007, 2975-2992.
4. T. Sakakura, J. C. Choi and H. Yasuda, *Chem. Rev.*, 2007, **107**, 2365-2387.
5. A. Behr, *Angew. Chem. Int. Ed.*, 1988, **27**, 661-678.
6. D. J. Darensbourg and R. A. Kudarowski, *Adv. Organomet. Chem.*, 1983, **22**, 129-168.
7. P. Braunstein, D. Matt and D. Nobel, *Chem. Rev.*, 1988, **88**, 747-764.
8. D. Walther, *Coord. Chem. Rev.*, 1987, **79**, 135-174.
9. W. Leitner, *Coord. Chem. Rev.*, 1996, **153**, 257-284.
10. G. Centi, E. A. Quadrelli and S. Perathoner, *Energy & Environmental Science*, 2013, **6**, 1711-1731.
11. R. Fornika and E. Dinjus, *Carbon Dioxide as C1-Building Block*, in "Applied Homogeneous Catalysis with Organometallic Compounds (B. Cornils, W.A. Herrmann, Eds), VCH, Weinheim, 1996, 1048-1071.
12. A. Goeppert, M. Czaun, G. K. S. Prakash and G. A. Olah, *Energy Environ. Sci.*, 2012, **5**, 7833-7853.
13. F. Asinger, *Methanol: Chemie- und Energierohstoff*, Springer-Verlag, Berlin, 1986.
14. A. Goeppert, G. K. S. Prakash and G. A. Olah, *Beyond Oil and Gas: The Methanol Economy*, WILEY-VCH, Weinheim, 2006.
15. M. Bertau, H. Offermanns, L. Plass, F. Schmidt and H.-J. Wernicke, *Springer, Berlin/Heidelberg*, 2014.
16. W. Wang, S. P. Wang, X. B. Ma and J. L. Gong, *Chem. Soc. Rev.*, 2011, **40**, 3703-3727.
17. <http://www.carbonrecycling.is/> (2014).
18. M. Behrens, F. Studt, I. Kasatkin, S. Kuhl, M. Havecker, F. Abild-Pedersen, S. Zander, F. Girgsdies, P. Kurr, B. L. Knip, M. Tovar, R. W. Fischer, J. K. Nørskov and R. Schlögl, *Science*, 2012, **336**, 893-897.
19. K. Tominaga, Y. Sasaki, T. Watanabe and M. Saito, *Bull. Chem. Soc. Jpn.*, 1995, **68**, 2837-2842.
20. S. Chakraborty, J. Zhang, J. A. Krause and H. R. Guan, *J. Am. Chem. Soc.*, 2010, **132**, 8872-+.
21. E. Balaraman, C. Gunanathan, J. Zhang, L. J. W. Shimon and D. Milstein, *Nature Chem.*, 2011, **3**, 609-614.
22. E. Balaraman, Y. Ben-David and D. Milstein, *Angew. Chem. Int. Ed.*, 2011, **50**, 11702-11705.
23. C. A. Huff and M. S. Sanford, *J. Am. Chem. Soc.*, 2011, **133**, 18122-18125.
24. S. Wesselbaum, T. vom Stein, J. Klankermayer and W. Leitner, *Angew. Chem. Int. Ed.*, 2012, **51**, 7499-7502.
25. H. T. Teunissen and C. J. Elsevier, *Chem. Commun.*, 1998, 1367-1368.
26. T. vom Stein, T. Weigand, C. Merckens, J. Klankermayer and W. Leitner, *ChemCatChem*, 2013, **5**, 439-441.
27. F. M. A. Geilen, B. Engendahl, A. Harwardt, W. Marquardt, J. Klankermayer and W. Leitner, *Angew. Chem. Int. Ed.*, 2010, **49**, 5510-5514.
28. F. M. Geilen, B. Engendahl, M. Hölscher, J. Klankermayer and W. Leitner, *J. Am. Chem. Soc.*, 2011, **133**, 14349-14358.
29. J. Coetzee, D. L. Dodds, J. Klankermayer, S. Brosinski, W. Leitner, A. M. Slawin and D. J. Cole-Hamilton, *Chemistry*, 2013, **19**, 11039-11050.
30. M. Nielsen, E. Alberico, W. Baumann, H. J. Drexler, H. Junge, S. Gladiali and M. Beller, *Nature*, 2013.
31. S. I. Hommeltoft and M. C. Baird, *Organometallics*, 1986, **5**, 190-195.
32. K. Tominaga and Y. Sasaki, *J. Mol. Catal. A: Chem.*, 2004, **220**, 159-165.
33. N. Sieffert, R. Reocreux, P. Lorusso, D. J. Cole-Hamilton and M. Buhl, *Chem. Eur. J.*, 2014, **20**, 4141-4155.
34. B. D. Yeomans, D. G. Humphrey and G. A. Heath, *J. Chem. Soc., Dalton Trans.*, 1997, 4153-4166.
35. K. M. Sung, S. Huh and M. J. Jun, *Polyhedron*, 1999, **18**, 469-479.
36. O. R. Allen, S. J. Dalgarno, L. D. Field, P. Jensen and A. C. Willis, *Organometallics*, 2009, **28**, 2385-2390.
37. I. Mellone, M. Peruzzini, L. Rosi, D. Mellmann, H. Junge, M. Beller and L. Gonsalvi, *Dalton Trans.*, 2013, **42**, 2495-2501.
38. M. K. Whittlesey, R. N. Perutz and M. H. Moore, *Organometallics*, 1996, **15**, 5166-5169.
39. I. S. Kolomnikov, A. I. Gusev, G. G. Aleksandrov, T. S. Lobeveva, Y. T. Struchkov and M. E. Volpin, *J. Organomet. Chem.*, 1973, **59**, 349-351.
40. M. G. Bradley, D. A. Roberts and G. L. Geoffroy, *J. Am. Chem. Soc.*, 1981, **103**, 379-384.
41. C. Bianchini, A. Meli, S. Moneti and F. Vizza, *Organometallics*, 1998, **17**, 2636-2645.
42. A. D. Getty, C.-C. Tai, J. C. Linehan, P. G. Jessop, M. M. Olmstead and A. L. Rheingold, *Organometallics*, 2009, **28**, 5466-5477.
43. A. Urakawa, F. Jutz, G. Laurenczy and A. Baiker, *Chem. Eur. J.*, 2007, **13**, 3886-3899.
44. P. G. Jessop, F. Joo and C.-C. Tai, *Coord. Chem. Rev.*, 2004, **248**, 2425-2442.
45. A. B. Chaplin and P. J. Dyson, *Inorg. Chem.*, 2008, **47**, 381-390.
46. M. Hirano, R. Fujimoto, K. Hatagami, N. Komine and S. Komiya, *ChemCatChem*, 2013, **5**, 1101-1115.
47. J. M. Brown, I. Gridnev and J. Klankermayer, *Amplification of Chirality*, 2008, **284**, 35-65.
48. Y. Musashi and S. Sakaki, *J. Am. Chem. Soc.*, 2000, **122**, 3867-3877.
49. C. Fellay, N. Yan, P. J. Dyson and G. Laurenczy, *Chem. Eur. J.*, 2009, **15**, 3752-3760.
50. L. E. Heim, N. E. Schlörer, J.-H. Choi and M. H. G. Precht, *Nature Commun.*, 2014, **5**.
51. X. Yang, *ACS Catal.*, 2014, **4**, 1129-1133.
52. A. J. M. Miller, D. M. Heinekey, J. M. Mayer and K. I. Goldberg, *Angew. Chem. Int. Ed.*, 2013, **52**, 3981-3984.
53. S. Savourey, G. Lefevre, J. C. Berthet, P. Thuery, C. Genre and T. Cantat, *Angew. Chem. Int. Ed.*, 2014.
54. F. Hutschka, A. Dedieu and W. Leitner, *Angew. Chem. Int. Ed.*, 1995, **34**, 1742-1745.
55. F. Hutschka, A. Dedieu, M. Eichberger, R. Fornika and W. Leitner, *J. Am. Chem. Soc.*, 1997, **119**, 4432-4443.
56. V. I. Bakmutov, E. V. Bakmutova, N. V. Belkova, C. Bianchini, L. M. Epstein, D. Masi, M. Peruzzini, E. S. Shubina, E. V. Vorontsov and F. Zanobini, *Can. J. Chem.*, 2001, **79**, 479-489.
57. G. Verspui, G. Elbertse, F. A. Sheldon, M. A. P. J. Hacking and R. A. Sheldon, *Chem. Commun.*, 2000, 1363-1364.
58. K. Burgemeister, G. Francio, V. H. Gego, L. Greiner, H. Hugl and W. Leitner, *Chem. Eur. J.*, 2007, **13**, 2798-2804.